Phase coherent transport in hollow InAs nanowires

T. Wenz, M. Rosien, F. Haas, T. Rieger, N. Demarina, M. I. Lepsa, H. Lüth, D. Grützmacher, and Th. Schäpers

Citation: Applied Physics Letters **105**, 113111 (2014); doi: 10.1063/1.4896286
View online: http://dx.doi.org/10.1063/1.4896286
View Table of Contents: http://scitation.aip.org/content/aip/journal/apl/105/11?ver=pdfcov
Published by the AIP Publishing

Phase coherent transport in hollow InAs nanowires

T. Wenz,[1] M. Rosien,[1] F. Haas,[1] T. Rieger,[1] N. Demarina,[2] M. I. Lepsa,[1] H. Lüth,[1] D. Grützmacher,[1] and Th. Schäpers[1,a)]
[1]*Peter Grünberg Institute (PGI-9) and JARA-Fundamentals of Future Information Technology, Forschungszentrum Jülich GmbH, 52425 Jülich, Germany*
[2]*Peter Grünberg Institute (PGI-2) and JARA-Fundamentals of Future Information Technology, Forschungszentrum Jülich GmbH, 52425 Jülich, Germany*

(Received 31 July 2014; accepted 10 September 2014; published online 18 September 2014)

Hollow InAs nanowires are produced from GaAs/InAs core/shell nanowires by wet chemical etching of the GaAs core. At room temperature, the resistivity of several nanowires is measured before and after removal of the GaAs core. The observed change in resistivity is explained by simulating the electronic states in both structures. At cryogenic temperatures, quantum transport in hollow InAs nanowires is studied. Flux periodic conductance oscillations are observed when the magnetic field is oriented parallel to the nanowire axis. © *2014 AIP Publishing LLC*.
[http://dx.doi.org/10.1063/1.4896286]

Semiconductor nanowires have been proven to be very versatile elements for various applications in nanoscience. This includes novel concepts in nano- and optoelectronics, as well as in photovoltaics.[1–3] Above that, semiconductor nanowires can also be employed in circuits related to quantum information technology.[4] Initially, starting from bulk nanowires considerable progress has been made in recent years towards more complex objects, such as radial or axial heterostructure nanowires as well as doped structures.[3,5,6] Using radial heterostructures, tubular conductors have been realized by covering a highly resistive GaAs core nanowire by a conductive InAs shell.[7] Due to the tubular topology of the conductive channel a magnetic field oriented parallel to the nanowire axis causes flux periodic (Aharonov-Bohm type) conductance oscillations.[8–10]

Apart from compact nanowires it is also possible to fabricate hollow nanowires either grown directly by epitaxy[11] or by removing the core of a radial heterostructure nanowire by selective wet chemical etching.[12–14] We use the latter approach to fabricate hollow InAs nanowires on the basis of GaAs/InAs core/shell (cs) nanowires. The interesting question is, if electron transport or even quantum transport phenomena can be maintained in these structures even under conditions where the electrons in the InAs tube are exposed to an outer and inner surfaces. Furthermore, it needs to be clarified to which extent the band alignment at the inner surface affects the electron occupation. For this purpose, we measure the conductivity and simulate the electron concentration at room temperature before and after removal of the GaAs core. Afterwards we study transport at low temperatures to find out if quantum transport effects, such as the aforementioned flux-periodic conductance oscillations, can be maintained.

GaAs/InAs core/shell nanowires are grown by molecular beam epitaxy on (111)-oriented substrates (GaAs or Si) covered by a thin SiO_2 layer. Two sets of nanowires with different geometric dimensions are investigated in this study. The GaAs core is grown at a temperature of 600 °C (630 °C) with a Ga rate of 0.1 μm h^{-1} (0.2 μm h^{-1}) and an As_4 beam equivalent pressure of 1×10^{-6} Torr (1.2×10^{-5} Torr).[15] The growth time of the core is 120 min (20 min). The core diameter t_c is about 125 nm (50 nm). After the core growth, the catalyzing Ga droplet is consumed by As. Subsequently, for the growth of the InAs shell the temperature is lowered to 490 °C and the In flux corresponding to 0.1 μm h^{-1} is introduced to enable a vapor solid overgrowth of the GaAs core with InAs.[7,14] The As_4 beam equivalent pressure is set to 1×10^{-6} Torr. The shell thickness t_s of about 25 nm (15 nm) is obtained after 20 min (15 min). The lattice mismatch of around 7% between GaAs and InAs is accommodated by the introduction of misfit dislocation at the interface.

After growth, the nanowires are mechanically transferred to a highly n-doped Si(100) substrate covered with a 200 nm thick SiO_2 layer. The Si substrate can be used as a back-gate in field-effect transistor measurements. Using electron beam lithography contact fingers are defined. To achieve low-resistance ohmic contacts, Ar^+ sputtering is employed to remove the native oxide on the nanowire surface. Subsequently, a Ti/Au layer is evaporated as the contact material. In Fig. 1(a), a core/shell nanowire partially covered by a contact finger is shown.

After electrical characterization of the GaAs/InAs core/shell nanowires at room temperature, the GaAs core is

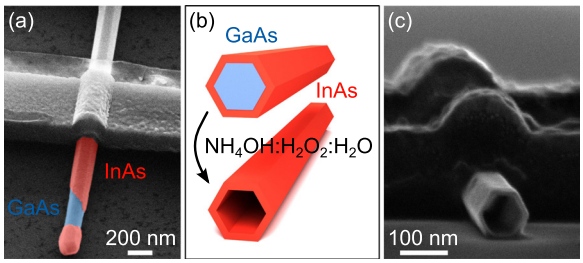

FIG. 1. (a) Scanning electron micrograph of a GaAs/InAs core/shell nanowire contacted with Ti/Au electrodes. In the front section, the core and shell are colored for clarity. (b) Schematic illustration: Selective etching with $NH_4OH:H_2O_2:H_2O$ removes the GaAs core. (c) Scanning electron micrograph of a contacted hollow InAs nanowire after the etching process.

a)Electronic mail: th.schaepers@fz-juelich.de

removed employing selective wet chemical etching, as illustrated in Fig. 1(b).[14] Using a solution of NH_3(aq)(25%):H_2O_2(30%):H_2O (1:1:30 in volume), a very high selectivity is obtained.[16] Figure 1(c) shows a contacted hollow InAs nanowire (hn).

The magnetotransport measurements are performed in a variable-temperature-insert at temperatures between 1.8 and 30 K using standard lock-in technique with 50 μV ac-bias voltage at 17.3 Hz and measuring current through the sample. The magnetic field is oriented along the nanowire axis. The samples are measured in a two-terminal configuration.

At room temperature, current-voltage (I-V) curves are taken for each GaAs/InAs core/shell nanowire. It is found that each curve is linear thus allowing for easy determination of the sample resistivity. Previous studies have shown contact resistances of InAs nanowires and GaAs/InAs core/shell nanowires to be small, when Ar^+ sputtering is employed,[7,17,18] which is why in the following we neglect the contact resistance. Figure 2 shows a map of the resistivity of the InAs shell before and after wet chemical etching of the two sets of nanowires. The range of measured resistivities before etching is in agreement with previous results.[7] In that study, it has been found that for core/shell nanowires with shell thicknesses $t_s > 12$ nm the resistivity only weakly depends on t_s which is confirmed here. A certain spread of resistivities between individual samples has been observed before for InAs nanowires grown by molecular beam epitaxy, c.f. Ref. 7.

As can be inferred from Fig. 2, after removal of the nanowire core the resistivity of the samples decreases. This is indicated by the fact that most dots are located below the diagonal line. Again, all I-V curves are linear. For $t_s = 15$ and 25 nm the resistivity decreased on average by a factor of roughly 2.8 and 2.3, respectively. For some nanowires, the opposite behavior is observed. It is possible that these samples were damaged during the etching process, which might increase the resistivity.

To explain the change in resistivity a simulation of the electronic states is carried out for a core/shell nanowire as well as for a hollow nanowire of the same dimensions using a self-consistent Schrödinger–Poisson solver. Here, the hexagonal cross-section of the nanowires was approximated by a circular one. Figure 3(a) shows the conduction band profile

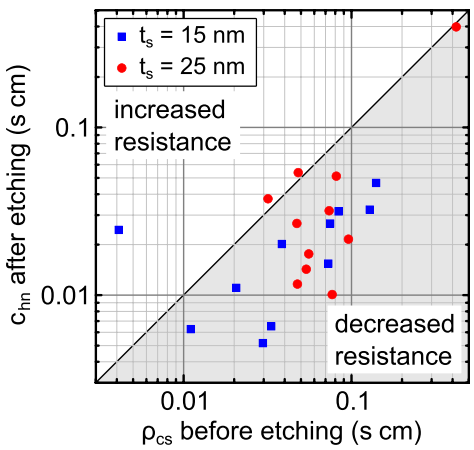

FIG. 2. Map of the resistivity before ρ_{cs} and after etching ρ_{hn} for several samples for shell thicknesses of $t_s = 15$ nm and 25 nm, respectively.

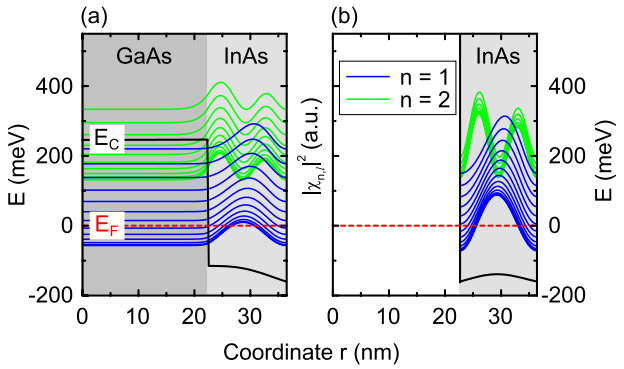

FIG. 3. Simulation of conduction band profile E_c and electronic states (a) of a GaAs/InAs core/shell nanowire and (b) of a hollow InAs nanowire with shell thickness $t_s = 13.7$ nm and core diameter $t_c = 22.7$ nm. Probability densities $|\chi_{n,l}(r)|^2$ as a function of radial position in the nanowire are shown for the first to subbands $n = 1$, 2 and the lowest angular momentum states l. The radial probability densities are offset to represent their respective energy relative to the Fermi energy $E_F = 0$. On the surfaces, the Fermi level is assumed to be pinned at 160 meV above the conduction band, leading to band bending. This causes more levels to be located below the Fermi level for the hollow InAs nanowire, as two surfaces are present.

E_c and the radial electron probability densities $|\chi_{n,l}(r)|^2$ for subbands $n = 1$, 2 and several angular momentum quantum numbers l for a structure comparable to the investigated set of nanowires with $t_s = 15$ nm and $t_c = 25$ nm.[19] Owing to the very high density of surface states at the InAs surface we assumed a pinning of the Fermi level at 160 meV above the conduction band edge.[20,21] In the present simulation, four angular momentum states of the first subband $n = 1$ are below the Fermi energy E_F and therefore populated. Please note that at zero magnetic field the energy levels are double and fourfold degenerate, for $l = 0$ and $|l| > 0$, respectively. The second subband $n = 2$ has a much higher energy and is therefore not occupied. The electron density in the shell can be calculated from the position of the electronic states and is found to be $n_{el,cs} = 4.95 \times 10^{17}\,cm^{-3}$.

The simulation is repeated for a hollow InAs nanowire with the same dimensions [cf. Fig. 3(b)]. Here, instead of the interface between GaAs and InAs, another InAs surface is present where the Fermi level is pinned. Due to the additional bending of the conduction band now two more fourfold-degenerate angular momentum states are below the Fermi level. This increases the electron density calculated for this structure to $n_{el,hn} = 6.27 \times 10^{17}\,cm^{-3}$. The increased electron density after removal of the GaAs core is the most probable explanation for the measured decrease in resistivity.

The simulation has also been carried out for structures corresponding to the second set of nanowires ($t_s = 25$ nm), where similar results have been found. For this structure, the electron concentration in the shell increases from $n_{el,cs} = 3.36 \times 10^{17}\,cm^{-3}$ to $n_{el,hn} = 6.11 \times 10^{17}\,cm^{-3}$. The conductivity increase by a factor of 2.3 as found in the experiment is in rough agreement.

In the following, low temperature quantum transport in a hollow InAs nanowire with shell thickness $t_s = 25$ nm and inner diameter $t_c = 125$ nm is discussed. Similar to the previous studies on GaAs/InAs core/shell nanowires[7,10] and on InAs/InAlAs core/shell nanowires,[9] the magnetic field is aligned along the nanowire axis [c.f. Fig. 4(c), inset]. These

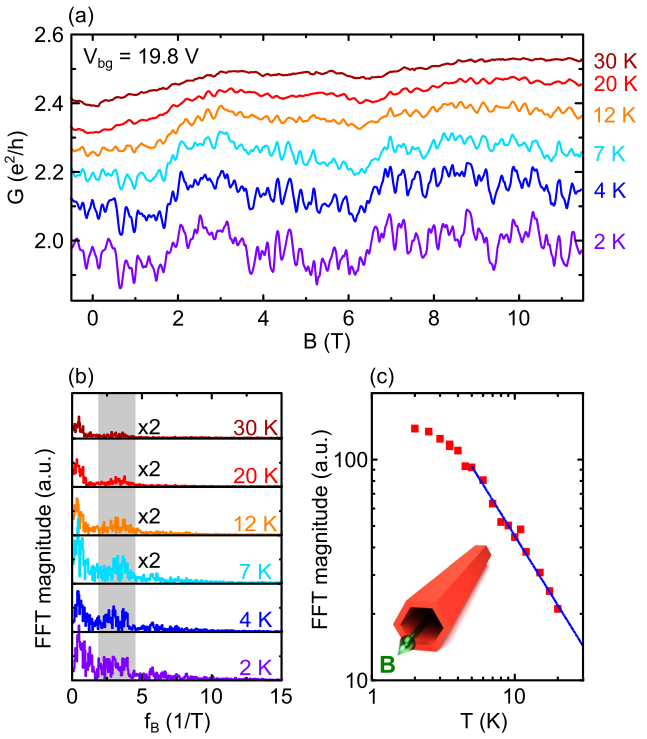

FIG. 4. (a) Magnetoconductance G in units of e^2/h with the magnetic field oriented in parallel to the nanowire axis for different temperatures. A backgate voltage of $V_{bg} = 19.8$ V has been applied. (b) FFT of the magnetoconductance measurements after subtraction of a broad background. The frequencies shaded in gray correspond to the expected frequency range based on the nanowire dimensions. (c) FFT peak intensity after summation over the shaded frequency range in (b) as a function of temperature. The blue line is a fit to the data according to T^{-a}. The inset illustrates the magnetic field orientation with respect to the nanowire axis.

studies have shown that in such tubular conductors the magnetoconductance G is periodic with the magnetic field period Φ_0/A. Here, $\Phi_0 = e/h$ is the magnetic flux quantum with e the electron charge and h the Planck constant and A is the area that is penetrated by the flux. Due to a small misalignment of the sample in the chip carrier, the nanowire axis is slightly tilted by about 11° with respect to the magnetic field. In order to obtain a linear current-voltage characteristics, a back-gate voltage of $V_{bg} = 19.8$ V was applied to increase the carrier concentration.

In Fig. 4(a), the magnetoconductance is shown for different temperatures between 2 and 30 K. The conductance fluctuates as a function of magnetic field, while the oscillation amplitude decreases with increasing temperature. Periodicity of the recorded data is not instantly apparent. For that purpose, the fast Fourier transform (FFT) of each curve has been calculated [cf. Fig. 4(b)]. Prior to that, a broad background is subtracted. The frequency range shaded in gray corresponds to the allowed frequency range for flux quantum periodicity, as given by the nanotube dimensions. The upper frequency corresponds to the area enclosed by the outer surface of the hollow InAs nanowire, while the lower frequency corresponds to the area enclosed by the inner surface. For all temperatures up to 20 K, a peak in the shaded region indicates the occurrence of flux periodic conductance oscillations.

At significantly lower frequencies an additional contribution due to conductance fluctuations is also visible in the FFT spectrum, probably a remainder of the imperfect subtraction of the background signal. In a recent theoretical calculation, it has been shown that these low frequency conductance fluctuations can originate from phase coherent transport in a disordered conductor.[22] The disorder might be due to impurities or due to potential fluctuations on the inner and outer surfaces. While the remaining background can be clearly separated from the flux periodic oscillations for temperatures larger than 4 K, the same is impossible for 2 K. We assume that for temperatures in the region of 2 K the highest contributing frequency of the fluctuations is in the range of the flux periodic frequencies due to the enhanced phase coherence length. As can be inferred from Fig. 4(b), when the temperature is increased, the highest frequency of the background fluctuations decreases, while the frequency of the flux periodic oscillations remains constant. Therefore, for temperatures of 4 K and higher, the two contributions can be clearly separated in the FFT spectrum.

For further analysis, the FFT magnitude has been summed over the region marked in gray for each temperature, as a measure for how the amplitude of the flux periodic oscillations develops as a function of temperature, c.f. Figure 4(c). For temperatures where the flux periodic contributions can be clearly separated from the background, a decay according to $\propto T^{-a}$ is observed, as indicated by the blue line in Fig. 4(c). The calculated exponent is $a = 1.04 \pm 0.05$. Possibly, this decay can be attributed to a loss of phase coherence,[23] i.e., by electron-electron scattering.

To investigate the dependence of the flux-periodic conductance oscillations on the electrostatic potential, the measurement is carried out at 1.8 K for several backgate voltages. Typical results are shown in Fig. 5(a). It is apparent that a change in backgate voltage alters the shape of the magnetoconductance curves. To investigate the influence on the flux periodic oscillations, the FFT of the data is calculated, as shown in Fig. 5(b). Again, contributions inside the expected frequency range (shaded region) are visible. Interestingly, their heights and shapes do not resemble. While a sharp peak is found for 19.4 V, the contributions to the flux periodic conductance oscillations are rather broadly distributed for 19.2 V. We assume that the potential landscape along the nanowire is non-uniform because of defects

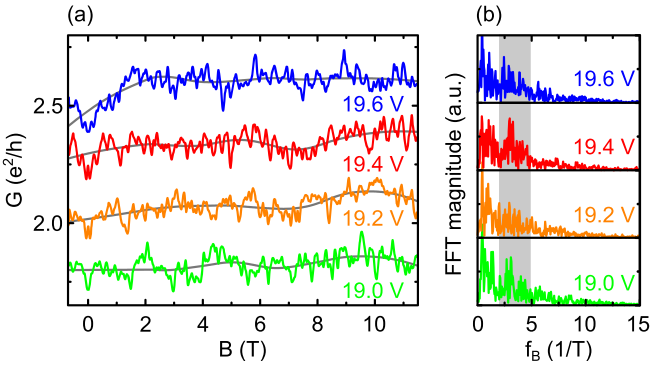

FIG. 5. (a) Magnetoconductance at $T = 1.8$ K with the magnetic field oriented parallel to the nanowire axis for different backgate voltages. Data are offset by 0.25 e^2/h. The gray lines indicate the broad background that is subtracted from the data prior to calculation of the FFT. (b) FFT of the magnetoconductance measurements after subtraction of a broad background. The frequencies shaded in gray correspond to the expected frequency range based on the nanowire dimensions.

on the substrate and the nanowire surface. Therefore, a change in backgate voltage can drastically alter the local electrostatic potential, which in turn seems to modify the shape of the flux periodic conductance oscillations.

In summary, hollow InAs nanowires were produced from molecular beam epitaxy grown GaAs/InAs core/shell nanowires by removing the GaAs core using wet chemical etching. The resistance of the hollow InAs nanowires is lower when compared to the GaAs/InAs core/shell nanowires before etching. This is explained with the help of a simulation of the electronic states in both structures. Studies at cryogenic temperatures reveal that flux periodic conductance oscillations can be observed in a hollow InAs nanowire, indicating that phase coherent transport is possible in such structures.

The authors are grateful to S. Trellenkamp for electron beam writing, S. Heedt and A. Manolescu for fruitful discussions, and H. Kertz and Ch. Krause for technical assistance.

[1]L.-E. Wernersson, C. Thelander, E. Lind, and L. Samuelson, Proc. IEEE **98**, 2047 (2010).
[2]C. M. Lieber, MRS Bull. **36**, 1052 (2011).
[3]K. A. Dick and P. Caroff, Nanoscale **6**, 3006 (2014).
[4]S. M. Frolov, S. R. Plissard, S. Nadj-Perge, L. P. Kouwenhoven, and E. P. A. M. Bakkers, MRS Bull. **38**, 809 (2013).
[5]J. K. Hyun, S. Zhang, and L. J. Lauhon, Annu. Rev. Mater. Res. **43**, 451 (2013).
[6]M. de la Mata, X. Zhou, F. Furtmayr, J. Teubert, S. Gradecak, M. Eickhoff, A. Fontcuberta i Morral, and J. Arbiol, J. Mater. Chem. C **1**, 4300 (2013).
[7]C. Blömers, T. Rieger, P. Zellekens, F. Haas, M. I. Lepsa, H. Hardtdegen, O. Gül, N. Demarina, D. Grützmacher, H. Lüth, and Th. Schäpers, Nanotechnology **24**, 035203 (2013).
[8]T. Richter, Ch. Blömers, H. Lüth, R. Calarco, M. Indlekofer, M. Marso, and Th. Schäpers, Nano Lett. **8**, 2834 (2008).
[9]G. W. Holloway, D. Shiri, C. M. Haapamaki, K. Willick, G. Watson, R. R. LaPierre, and J. Baugh, e-print arXiv:1305.5552 [cond-mat.mes-hall] (2013).
[10]O. Gül, N. Demarina, C. Blömers, T. Rieger, H. Lüth, M. I. Lepsa, D. Grützmacher, and Th. Schäpers, Phys. Rev. B **89**, 045417 (2014).
[11]E. P. A. M. Bakkers and M. A. Verheijen, J. Am. Chem. Soc. **125**, 3440 (2003).
[12]P. Mohan, J. Motohisa, and T. Fukui, Appl. Phys. Lett. **88**, 013110 (2006).
[13]R. E. Algra, M. Hocevar, M. A. Verheijen, I. Zardo, G. G. W. Immink, W. J. P. van Enckevort, G. Abstreiter, L. P. Kouwenhoven, E. Vlieg, and E. P. A. M. Bakkers, Nano Lett. **11**, 1690 (2011).
[14]T. Rieger, M. Luysberg, Th. Schäpers, D. Grützmacher, and M. I. Lepsa, Nano Lett. **12**, 5559 (2012).
[15]T. Rieger, S. Heiderich, S. Lenk, M. I. Lepsa, and D. Grützmacher, J. Cryst. Growth **353**, 39 (2012).
[16]D. G. Hill, K. L. Lear, and J. S. Harris, J. Electrochem. Soc. **137**, 2912 (1990).
[17]C. Blömers, M. I. Lepsa, M. Luysberg, D. Grützmacher, H. Lüth, and Th. Schäpers, Nano Lett. **11**, 3550 (2011).
[18]M. J. L. Sourribes, I. Isakov, M. Panfilova, and P. A. Warburton, Nanotechnology **24**, 045703 (2013).
[19]The shown simulation is carried out for structures with a round footprint ($t_s = 13.7$ nm and $t_c = 22.7$ nm), whereas the actual nanowires have a hexagonal shape. The calculated structure corresponds to a hexagonal nanowire with $t_s = 15$ nm and core diameter $t_c = 25$ nm. Simulation parameters for the other set of nanowires are adjusted accordingly.
[20]K. Smit, L. Koenders, and W. Mönch, in Proceedings of the 16th Annual Conference on the Physics and Chemistry of Semiconductor Interfaces (1989), Vol. 7, p. 888.
[21]H. Lüth, *Solid Surfaces, Interfaces and Thin Films*, Graduate Texts in Physics (Springer Berlin Heidelberg, 2010).
[22]T. O. Rosdahl, A. Manolescu, and V. Gudmundsson, Phys. Rev. B **90**, 035421 (2014).
[23]J. J. Lin and J. P. Bird, J. Phys.: Condens. Matter **14**, R501 (2002).